

# Optimal Generator Start-up Sequence for Bulk System Restoration with Active Distribution Networks

**Zhao, Jin; Wang, Hongtao ; Wu, Qiuwei; Hatziargyriou, Nikos D.; Shen, Feifan**

*Published in:*
IEEE Transactions on Power Systems

*Link to article, DOI:*
10.1109/TPWRS.2020.3040130

*Publication date:*
2021

*Document Version*
Peer reviewed version

# Optimal Generator Start-up Sequence for Bulk System Restoration with Active Distribution Networks

Jin Zhao, *Student Member*, Hongtao Wang, *Senior Member*, Qiuwei Wu, *Senior Member*, *IEEE*, Nikos D. Hatziargyriou, *Fellow*, *IEEE*, Feifan Shen *Student Member*.

***Abstract*—This paper proposes a new scheme for bulk system restoration considering the available black-start resources (BSRs) in the distribution system (DS). The DS assisted generator start-up sequence (D-GSS) scheme is realized in a decentralized way, so that it does not only benefit the bulk system GSS by utilizing available BSRs in the DS, but also respects the independent operation of the transmission system operator (TSO) and distribution system operators (DSOs). First, the decentralized D-GSS scheme is presented including the interaction of the TSO and DSOs and the corresponding compact models. The models of the decentralized D-GSS scheme are built with the bulk system GSS modeled as a mixed-integer quadratic program (MIQP), the DS multi-step operation modeled as mixed-integer second-order conic programs (MISOCPs) and reliable power supply assessments of renewable energy sources as linear programs (LPs). Finally, a projection function based analytical target cascading (P-ATC) method is developed to iteratively solve the decentralized models with model complexity reduction. The P-ATC algorithm can handle integer variables and improve the computational efficiency of the iterative calculation process. The effectiveness of the proposed method is validated using the small-scale T6D2 system and large-scale T118D5 system, showing good GSS performance and computation efficiency.**

***Index Terms*—Distributed optimization, generator start-up, transmission and distribution system, power system resilience.**

## NOMENCLATURE

### A. Abbreviations

| | |
|---|---|
| BSG | Black-start generator. |
| NBSG | Non-black-start generator. |
| BSR | Black-start resources. |
| GSS | Generator start-up sequence. |
| TS | Transmission system. |
| DS | Distribution system. |
| RES | Renewable energy source. |
| DG | Distributed generator. |
| ES | Energy storage. |
| TSO | Transmission system operator. |
| DSO | Distribution system operator. |

### B. Index

| | |
|---|---|
| $i$ | Index of nodes. |
| $j$ | Index of DS. |
| $t$ | Index of stage. |
| $k$ | Index of iteration. |
| P | Index for projection related variables. |

### C. Parameters

| | |
|---|---|
| $v_j$, $w_j$ | Penalty multipliers of augmented Lagrangian relaxation. |
| $P_{G,i}^{max}$ | Maximum output power of generator $i$. |
| $P_{G,i}^{crk}$ | Required restart power of generator $i$. |
| $R_{G,i}$ | Ramp-up rate of generator $i$. |
| $T_{crk,i}$ | Cranking time of generator $i$. |
| $T_{R,i}$ | Ramping time of generator $i$. |
| $T_{H,max,i}$ | Critical maximum time interval for NBS $i$. |
| $T_{C,min,i}$ | Critical minimum time interval for NBS $i$. |
| $M$ | Constant with large enough value. |
| $X_{mn}$, $R_{mn}$ | Reactance and resistance of branch $mn$. |
| $C_j$ | Allowed switching action number for DS $j$ in the restoration period $T$. |
| $P_{CH,m,max}$, $P_{DC,m,max}$ | Active power limits of ES charging and discharging modes at node $m$. |
| $\lambda_{DC,m}$, $\lambda_{CH,m}$ | Charging/discharging efficiency of ES. |
| $C_{ES,m}$ | Capacity of ES. |

### D. Variables

| | |
|---|---|
| $P_{TB,j}$, $P_{DB,j}$ | TS power demand and DS power supply between the TS and DS $j$. |
| $\sigma_j$ | TD boundary power mismatch value. |
| $E_{gen,i}$ | Generation capability of generator $i$. |
| $\boldsymbol{t}_{G,sta}$ | Vector of the generator restart time. |
| $\boldsymbol{u}_G$, $\boldsymbol{u}_{Line}$ | Vectors of auxiliary variables for generator ramp-up model and buses and lines energization. |
| $\boldsymbol{p}_{RE}$ | Vector of RES output at the TS level. |
| $\boldsymbol{P}_{TB}$ | Vector of TD boundary power demand at the TS level. |
| $P_{TB,j}$, $P_{DB,j}$ | TS power demand and DS power supply between the TS and DS $j$. |
| $\boldsymbol{\beta}_j$ | Vectors of line switch binary variables. |
| $\boldsymbol{u}_{DS,j}$ | Vectors of auxiliary variables for the DS topology. |
| $\boldsymbol{x}_{L,j}$ | Vectors of load pickup decision variables. |
| $\boldsymbol{p}_{DG,j}$ | Vectors of RES-DG output variables. |
| $\boldsymbol{p}_{ESS,j}$ | Vectors of ES dispatch variables. |

This work was supported by the Science and Technology Foundation of SGCC (Research on Key Sub-station Control Technology for Rapid Recovery of AC/DC Hybrid Power Grid) (SGSDDK00KJJS1800084), (*Corresponding author*: Hongtao Wang; Qiuwei Wu).

J. Zhao and H. Wang are with the Key Laboratory of Power System Intelligent Dispatch and Control of Ministry of Education, Shandong University, Jinan 250000, China. (e-mail: hizhaojin@163.com; whtwhm@sdu.edu.cn).

Q. Wu and F. Shen are with the Center for Electric Power and Energy, Department of Electrical Engineering, Technical University of Denmark, Kgs. Lyngby, DK 2800 (e-mail: qw@elektro.dtu.dk; fshen@elektro.dtu.dk).

N. D. Hatziargyriou is with the National Technical University of Athens, Athens 15773, Greece (e-mail: nh@power.ece.ntua.gr).

$t_{sta,i}$ Restart time step of generator $i$.
$O^s_{i,t}$ Binary variable to represent the state of stage $s$ of generator $i$ in restoration step $t$.
$Z^s_{i,t}$, $A^s_{a,i,t}$, $A^s_{b,i,t}$ Auxiliary variables to handle absolute values.
$P_{G,i,t}$ Generator output of generator $i$ at step $t$.
$y_{i,t}$ Uncertain variable of node $i$ at step $t$.
$u_{C,I}$, $u_{H,i}$ Auxiliary binary variables for critical time interval limits.
$u_{bus,i,t}$, $u_{Line,l,t}$, $u_{bus,m,t}$, $u_{bus,n,t}$ Binary variables for generator connected node $i$, transmission line $l$ and nodes $m$ and $n$ connected to line $l$.
$P_{G,m,t}$, $Q_{G,m,t}$ Active and reactive power injection of DS node $m$.
$P_{DL,m,t}$, $Q_{DL,m,t}$ Active and reactive load of DS node $m$.
$x_{DL,m,t}$ Binary variable for load pickup decision of DS node $m$.
$P_{mn,t}$, $Q_{mn,t}$ Active and reactive power flow from node $m$ to node $n$.
$V^{sqr}_{m,t}$, $V^{sqr}_{n,t}$ Square voltage magnitude at node $m$ and node $n$.
$I^{sqr}_{mn,t}$ Square current magnitude from node $m$ to $n$.
$\alpha_{j,mn,t}$ Auxiliary binary variable for switching action of DS $j$ branch $mn$ at step $t$.
$Z_{j,mn,t}$ Continuous variable for the on/off status of branch $mn$.
$\beta_{mn,t}$, $\beta_{nm,t}$ Binary auxiliary variables associated with the existence of power flows from node $m$ to node $n$.
$P_{ES,m,t}$ Active power output of ES connected to node $m$.
$x_{CH,m,t}$, $x_{DC,m,t}$ Binary variables for charging and discharging states of ES at node $m$ at step $t$.
$E_{ES,m,t}$ Energy reservoir for ES node $m$ at step $t$.

## I. Introduction

POWER system restoration (PSR) is the process of bringing the system back to normal operation after a partial or complete blackout [1]. The increasing complexities and uncertainties of modern power systems make the fast PSR an indispensable part for system hardening and operational enhancement [2]. Restoration heavily relies on the available power supply in the system. Most of generating units do not have self-starting capabilities [3]. Therefore, in the early stages of restoration, BSGs are used to supply cranking power to NBSGs [4]. With limited BSRs in the power system, generators should be re-started sequentially to optimally exploit the available black-start power [3], [5]. In [3], the start-up sequencing problem of NBSGs is considered to optimize the BSR allocation. Ref. [6] proposed a knowledge-based approach to optimize the GSS by maximizing the served load. Ref. [7] built a highly efficient mixed-integer linear programming (MILP) model for the GSS optimization. The GSS model was constructed in [8] to maximize the overall system generated power with the optimal power system topology.

In general, bulk system generator start-up relies on conventional BSRs, such as hydro and thermal units [9], and studies are normally conducted at the TS level [6]-[11]. Recently, RESs can be also considered as BSRs, since their controllability has been largely improved. A control method to enable wind turbines to provide black-starting capacity was proposed in [10]. Ref. [11] coordinated wind farms and pumped-storage hydro units to benefit the generator start-up process. Taking micro-grids as BSRs, the GSS optimization was studied in [12]. Next to large-scale wind farms at the TS level, most of RESs are today integrated in DSs, as DGs [13]. RES-based DGs and ES, as new types of BSRs at the DS, can support the restoration process by providing more power for generator restarting in the early restoration steps. Therefore, the conventional GSS can be improved by utilizing BSRs at the DS.

The limited amount of information exchanged between the TSO and the DSOs hinders the utilization of the DS BSRs in the overall system black-start process. In fact, in deregulated systems, the TSO and DSOs are independent companies and have little knowledge of each other's networks [14], [15]. This hinders the centralized optimization considering BSRs in DSs in order to contribute to the bulk system NBSGs start-up. Using decentralized methods, the independent operation of the TSO and DSOs is respected, while by exchanging boundary information at the substations between TS and DSs [16], their coordination for better bulk system GSS with more available generation at each step can be achieved. Since, a high reliability is requested from BSRs [1], the uncertainty of RESs should be considered to ensure reliable power supply for the generator restart process.

Decentralized PSR methods rely on decentralized algorithms. The analytical target cascading (ATC) method is a model-based decentralized algorithm for multilevel hierarchical optimization problems and has good convergence performance even for non-convex models [17]. In [14], [16]-[18], the ATC method realizes decentralized unit commitment, decentralized load restoration and decentralized operation of the AC/DC system. Ref. [19]-[20] propose ATC based voltage control methods, which are very helpful for dispatching large-scale wind farm clusters. For the GSS problem considering DS operations, tremendous binary variables are integrated in decentralized models. In order to mitigate the computational burden of the ATC based iterative calculation process, the projection method [21] is used to handle binary variables. Accordingly, a projection function based analytical target cascading (P-ATC) algorithm is developed to efficiently deal with non-continuous variables in decentralized models.

In this paper, a DS assisted GSS (D-GSS) scheme is proposed based on an improved decentralized optimization method. First, the framework of bulk system GSS with active DSs is presented. Then, the detailed models of the GSS problem in the TS, the BSR support at the DS level and the reliable power supply assessment of uncertain RESs are constructed. Finally, a P-ATC algorithm is developed to handle the complex DS multi-step operation models considering dispatch of DGs and ESs dispatch, pickup of critical loads and network configura-

tion. Results are obtained by iteratively solving the decoupled models of the TSO and DSOs.

The contributions of this paper are threefold. 1) A new D-GSS scheme is proposed considering the support from BSRs in the DSs, and coordinating the D-GSS process with the independent decision-making of the TSO and DSOs. 2) The corresponding models are built with tractable computation. The decentralized GSS model in the TS is constructed as mixed-integer quadratic program (MIQP). Decentralized DS operation models with configuration, which consider power demand of TS generator start-up and DS critical load recovery, are constructed as mixed-integer second-order conic program (MISOCP). The reliable available generation assessment of uncertain BSRs is constructed as linear program (LP). 3) An efficient algorithm, the P-ATC, is developed to solve decentralized D-GSS models. It handles the complex multi-step decentralized models in the TS and DSs by parallel calculation and integer variables reduction. With highly efficient computation, the P-ATC algorithm can realize the application of the D-GSS scheme in the on-line restoration process.

The rest of the paper is organized as follows. Section II introduces the framework of optimal GSS considering parallel DSs. The detailed decentralized models are constructed in Section III. Section IV presents the iterative calculation process of the improved algorithm. Section V provides case studies, followed by conclusions.

## II. Framework of D-GSS scheme

This section provides an overview of the bulk system GSS problem considering parallel DSs. The structure of the coupled TS and DS systems is presented with their internal components. Compact decentralized models are derived to realize the coordination and independent operation of the different system operators.

### A. GSS oriented coordination of TSO and DSOs

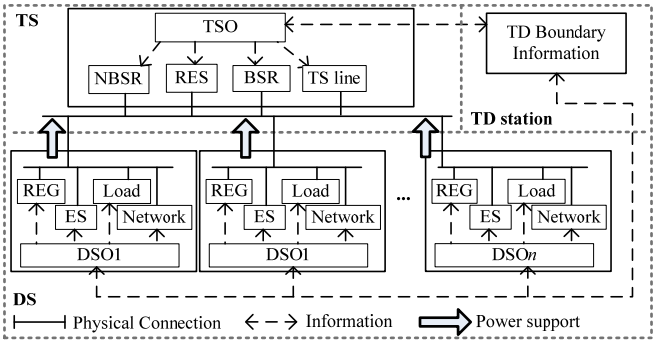


Fig. 1. Bulk system generator startup with parallel DSs

Generating units can be divided into BSGs and NBSGs. The BSGs can start on their own, while NBSGs require external cranking power. The aim of the GSS optimization is to maximize the overall system generation capability during a multi-step restoration period [6]-[8], [12]. Fig. 1 shows a system, where a TSO and several DSOs participate in the D-GSS scheme. The generating resources at the TS level, such as NBSGs, conventional BSGs and large-scale RESs, are dispatched by the TSO. RES-DGs, ESs, DS loads and switches in each DS are managed by the respective DSO. The DSs in Fig. 1 are the ones with the ability to assist the generator start-up process. They still have available power supply after their internal critical loads are energized.

In the following, the system operators are coordinated in a decentralized way aiming at optimal bulk system GSS. Fig. 2 shows the process to obtain the optimal decentralized D-GSS. First, the TSO and DSOs check the systems conditions, i.e. available BSRs, bus and line energization status and reliable power supply from uncertain sources, in order to prepare the parameters for the corresponding optimization models. Then, the TSO performs GSS optimization considering DSs assistance specified by power demand at the boundary transmission and distribution (TD) substations. Using the boundary information at TD substations, each DSO dispatches his resources and adjusts the network configuration in order to provide power support through the TD substation. The power supply from DSs may not meet the TSO expectation due to limited available BSRs and security constraints at DS levels. Nevertheless, the available power supplies from DSs are submitted to the TSO forcing him to adjust the GSS scheme and update the boundary power demand. This leads to another round of internal dispatch by the DSO. The interaction of system operators continues until boundary power demands of the TSO and power supplies of DSOs converge. This process is realized through iterative model optimization of the TSO and DSOs at each step providing the D-GSS strategy for multi-step restoration process.

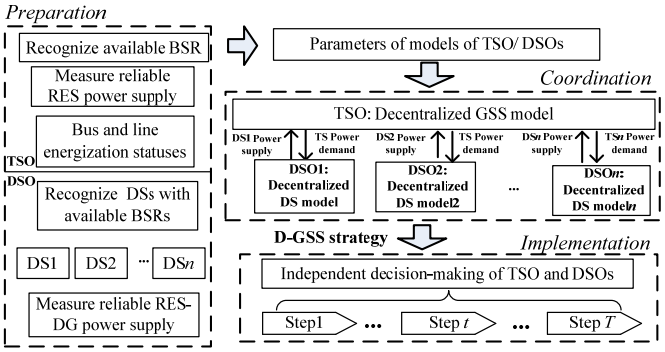


Fig. 2. Process to form the decentralized D-GSS scheme

### B. Compact decentralized models for TSO and DSOs

The key to building decentralized models is decoupling the TS and DS boundary variables between the TS and DSs. For the GSS problem, the boundary active power between TS and DS $j$ is decoupled using the augmented Lagrangian relaxation method [22]. The penalty function $\Phi(\ )$ in (1) relaxes the TD boundary power mismatch value $\sigma_j$ which is originally equal to 0. $N_{\mathrm{SUB}}$ is the sets of DSs. Parameters $v_j$ and $w_j$ will be updated during the iterative calculation process.

$$\begin{aligned} &\Phi_j\left(\boldsymbol{\sigma}_j\right)=v_j\sigma_j+\left\|w_j\circ\sigma_j\right\|_2^2 \\ &\sigma_j=P_{\mathrm{TB},j}-P_{\mathrm{DB},j}\quad(\forall j\in N_{\mathrm{SUB}}) \end{aligned} \tag{1}$$

Accordingly, the compact models of the decentralized D-GSS scheme are presented as (2)-(3).

$$\text{TSO}: \max\left(\sum_{i\in N_{\text{BS}}} E_{\text{gen},i} - \sum_{i\in N_{\text{NBS}}} E_{\text{gen},i}\right) - \sum_{j\in N_{\text{SUB}}} \Phi_j\left(\sigma_j\right)$$
$$\text{s.t.} \quad \boldsymbol{g}_{\text{TS}}(\boldsymbol{t}_{\text{G,sta}}, \boldsymbol{u}_{\text{G}}, \boldsymbol{u}_{\text{Line}}, \boldsymbol{p}_{\text{RE}}, \boldsymbol{P}_{\text{TB}}) \le 0 \qquad (2)$$
$$\boldsymbol{h}_{\text{TS}}(\boldsymbol{t}_{\text{G,sta}}, \boldsymbol{u}_{\text{G}}, \boldsymbol{u}_{\text{Line}}, \boldsymbol{p}_{\text{RE}}, \boldsymbol{P}_{\text{TB}}) = 0$$

$\boldsymbol{g}_{\text{TS}}(\ )$ and $\boldsymbol{h}_{\text{TS}}(\ )$ are the TS equality and inequality constraints including generator startup constraints, energization constraints and TD boundary power limits. $N_{\text{BS}}$ and $N_{\text{NBS}}$ are sets of BSG and NBSG.

$$\text{DSO } j: \min \Phi_j\left(\sigma_j\right)$$
$$\text{s.t.} \quad \boldsymbol{g}_{\text{DS},j}(\boldsymbol{\beta}_j, \boldsymbol{u}_{\text{DS},j}, \boldsymbol{x}_{\text{L},j}, \boldsymbol{p}_{\text{DG},j}, \boldsymbol{p}_{\text{ESS},j}, P_{\text{DB},j}) \le 0 \qquad (3)$$
$$\boldsymbol{h}_{\text{DS},j}(\boldsymbol{\beta}_j, \boldsymbol{u}_{\text{DS},j}, \boldsymbol{x}_{\text{L},j}, \boldsymbol{p}_{\text{DG},j}, \boldsymbol{p}_{\text{ESS},j}, P_{\text{DB},j}) = 0$$

$\boldsymbol{g}_{\text{DS},j}(\ )$ and $\boldsymbol{h}_{\text{DS},j}(\ )$ are network reconfiguration related constraints and security related constraints of DS $j$. The objective of each DS in (3) is to satisfy the TD boundary power, however other DS objectives, such as minimizing power loss, can be added as required by each DSO.

Model (2) is the decentralized GSS optimization conducted by the TSO and Model (3) is the decentralized multi-step operation model of DS $j$ considering configuration. Note that the TSO and DSO models are coupled because of the penalty function (1), and $p_{\text{RE}}$ and $p_{\text{DG}}$ are uncertain variables. By iterative calculation, these decentralized models can be decoupled and solved in parallel. The detailed model and reliable power supply assessment of uncertain BSRs are provided in section III. The decentralized optimization based on P-ATC method, which efficiently handles large numbers of integer variables, is shown in section IV.

## III. Models of Decentralized D-GSS Scheme

In this section, decentralized models of the TSO and DSOs corresponding to (1) and (2) are provided. Considering the generator restart model and TS bus/line energization constraints, the TSO model is formulated as a MILP. The DSO model is constructed as MISOCP considering network reconfiguration. The reliable power supplies of uncertain BSRs are measured with a defined confidence level using LP.

### *A. Decentralized D-GSS optimization model of TSO*

The restart characteristics of BSG and NBSG can be modeled as piecewise functions according to Fig. 3 [6]-[8]. BSGs can be restarted when needed, while NBSGs need cranking power to restart.

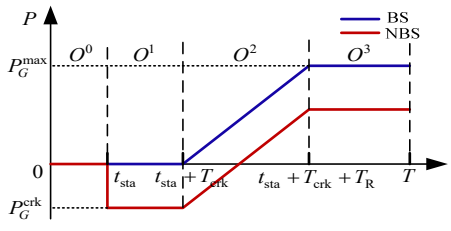


Fig. 3. Generation capability characteristics of generators

1) *Objective function*. The objective is to maximize the system generation capacity during the restoration time $T$. According to [6], the objective function can be equivalently simplified as the first term in (4). The second term of (4) is the penalty function related to the coupled TD boundary power.

$$\min \sum_{i\in N_{\text{NBR}}} \left(P_{\text{G},i}^{\max} - P_{\text{G},i}^{\text{crk}}\right) t_{\text{sta},i} + \sum_{j\in N_{\text{SUB}}} \left(\nu_j\left(\boldsymbol{P}_{\text{TB},j} - \boldsymbol{P}_{\text{DB},j}\right) + \left\| w_j \circ \left(\boldsymbol{P}_{\text{TB},j} - \boldsymbol{P}_{\text{DB},j}\right)\right\|_2^2\right) \qquad (4)$$

2) *Generator restart function*. The capacities of BSGs and NBSGs in a restoration period $T$ can be expressed as (5)-(16) by introducing four binary variables ($O^0$, $O^1$, $O^2$, $O^3$) for the four states at each step $t$ [12].

$$\sum_{s\in\{0,1,2,3\}} O_{i,t}^s = 1 \quad \forall i \in N_{\text{BS}} \bigcup N_{\text{NBS}}, t = \{1,...,T\} \qquad (5)$$

$$O_{i,t}^s \le O_{i,t+1}^s + O_{i,t+1}^{s+1} \quad \forall s \in [0,1,2] \quad \forall i \in N_{\text{BS}} \bigcup N_{\text{NBS}}, t = \{1,...,T-1\} \qquad (6)$$

$$O_{i,t}^3 \le O_{i,t+1}^3 \quad \forall i \in N_{\text{BS}} \bigcup N_{\text{NBS}}, t = \{1,...,T-1\} \qquad (7)$$

$$O_{i,0}^0 = 1 \quad \forall i \in N_{\text{NBS}} \qquad (8)$$

$$O_{i,t}^0 = 0 \quad \forall i \in N_{\text{BS}}, t = \{1,...,T-1\} \qquad (9)$$

$$O_{i,T}^3 = 1 \quad \forall i \in N_{\text{BS}} \bigcup N_{\text{NBS}} \qquad (10)$$

$$\sum_{t=1}^{T-1} \left|O_{i,t}^1 - O_{i,t+1}^1\right| = 2 \quad \forall i \in N_{\text{NBS}} \qquad (11)$$

$$\sum_{t=1}^{T-1} \left|O_{i,t}^1 - O_{i,t+1}^1\right| = 1 \quad \forall i \in N_{\text{BS}} \qquad (12)$$

$$\sum_{t=1}^{T-1} \left|O_{i,t}^2 - O_{i,t+1}^2\right| = 2 \quad \forall i \in N_{\text{NBS}} \bigcup N_{\text{BS}} \qquad (13)$$

$$\sum_{t=1}^{T} O_{i,t}^0 = t_{\text{sta},i} - 1 \quad \forall i \in N_{\text{BS}} \bigcup N_{\text{NBS}} \qquad (14)$$

$$\sum_{t=1}^{T} O_{i,t}^1 = T_{\text{crk},i} \quad \forall i \in N_{\text{BS}} \bigcup N_{\text{NBS}} \qquad (15)$$

$$\sum_{t=1}^{T} O_{i,t}^2 = P_{\text{G},i}^{\max} \Big/ R_{\text{G},i} = T_{\text{R},i} \quad \forall i \in N_{\text{BS}} \bigcup N_{\text{NBS}} \qquad (16)$$

The generator restart characteristics in Fig. 3 can be expressed by (5)-(16). Eq. (5) means the generator can only be in one of the four states ($O^0$, $O^1$, $O^2$ and $O^3$ in Fig. 3) in each step. Constraints (6)-(7) ensure that the state of generators changes from $O^0$ to $O^3$. The initial condition of PSR is set in (8) which means all the generators are off-line. Eq. (9) indicates BSGs can be self-restarted at any time, and (10) means all the generators are restored at the end step $T$. Eqs. (11)-(13) restrict state changes of generators in the restoration period $T$: states of NBSGs can move from $O^0$ to $O^1$ as well as from $O^1$ to $O^2$ in (11) while states of BSGs can only move from $O^1$ to $O^2$ in (12) because BSGs do not have state $O^0$ according to (9), and, in (13), states of NBSGs and BSGs can move from $O^1$ to $O^2$ and from $O^2$ to $O^3$. Each generator has the constraints of the start time (14), cranking time (15) and ramping time (16). The detailed explanation of these equations can be found in [12]. In order to handle the absolute values in (11)-(13), the auxiliary binary variables $Z_{i,t}^s = |O_{i,t}^s - O_{i,t+1}^s|$, $A_{a,i,t}^s$ and $A_{b,i,t}^s$ are introduced to transform (11)-(13) into linear forms using (17). Constraints in (17) replace absolute values in (11)-(13) with binary variable $Z_{i,t}^s$.

$$\begin{cases} 0 \le Z_{i,t}^{s} - \left(O_{i,t}^{s} - O_{i,t+1}^{s}\right) \le 2A_{a,i,t}^{s} \\ 0 \le Z_{i,t}^{s} - \left(O_{i,t+1}^{s} - O_{i,t}^{s}\right) \le 2A_{b,i,t}^{s} \\ A_{a,i,t}^{s} + A_{b,i,t}^{s} = 1 \quad s \in \{1,2\}, t = \{1,...,T-1\} \end{cases} \tag{17}$$

Accordingly, the output power of generator $i$ at step $t$ is represented in (18), and (18) is further transformed into the linear form (19) where binary variable $y_{i,t} = O_{i,t}^{2}\, O_{i,t}^{0}$ and $y_{i,t}$ satisfies (20).

$$\begin{aligned} P_{\mathrm{G},i,t} = &-\left(O_{i,t}^{1} + O_{i,t}^{2} + O_{i,t}^{3}\right) P_{\mathrm{G},i}^{\mathrm{crk}} + O_{i,t}^{2} R_{\mathrm{G},i}\left(t - t_{\mathrm{sta},i} + 1 - T_{i}^{\mathrm{crk}}\right) \\ &+ O_{i,t}^{3} P_{\mathrm{G},i}^{\max} \qquad \forall i \in N_{\mathrm{BS}} \bigcup N_{\mathrm{NBS}}, t = \{1,...,T\} \end{aligned} \tag{18}$$

$$\begin{aligned} P_{\mathrm{G},i,t} = &-\left(O_{i,t}^{1} + O_{i,t}^{2} + O_{i,t}^{3}\right) P_{\mathrm{G},i}^{\mathrm{crk}} + O_{i,t}^{2} R_{\mathrm{G},i}\left(t - T_{i}^{\mathrm{crk}}\right) - R_{\mathrm{G},i} \sum_{t=0}^{T} y_{i,t} \\ &+ O_{i,t}^{3} P_{\mathrm{G},i}^{\max} \qquad \forall i \in N_{\mathrm{BS}} \bigcup N_{\mathrm{NBS}}, t = \{1,...,T\} \end{aligned} \tag{19}$$

$$\begin{cases} y_{i,t} \ge O_{i,t}^{0} + O_{i,t}^{2} - 1 \\ y_{i,t} \le O_{i,t}^{0}, y_{i,t} \le O_{i,t}^{2} \\ \forall i \in N_{\mathrm{BS}} \bigcup N_{\mathrm{NBS}}, t = \{1,...,T\} \end{cases} \tag{20}$$

In this way, the BSG/NBSG restart function can be expressed in a linearized form using (5)-(17) and (19)-(20).

3) *RES-BSR output assessment*. Since the generator startup process requires reliable BS capacity, the uncertain nature of RES BSRs should be carefully considered. Therefore, the conditional value-at-risk (CVaR) method [23] is used to ensure RESs provide reliable power supply with a defined confidence level. CVaR values of RES outputs are integrated in the GSS model as available generation of RES-BSRs. As Fig. 4 shows, the CVaR value provides reliable generation assessment of uncertain BSRs and can be adjusted flexibly according to actual restoration conditions.

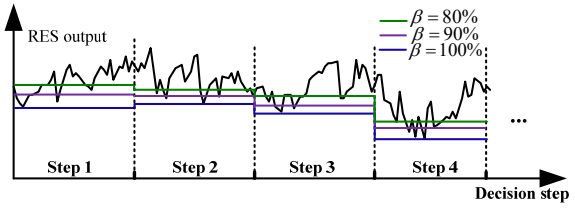


Fig. 4. CVaR values of RES output with different confidence levels

The uncertain power injection of RES connected to bus $i$ is formulated as (21) which is the sum of predicted value $E_{F,i,t}$ and predicted error $y_{\mathrm{error},i,t}$ at step $t$. $\rho(y_{i,t})$ is the probability density function of uncertain power $y_{i,t}$. The probability of the uncertain variable $y_{i,t}$ not exceeding the threshold $\alpha$ is (22).

$$y_{i,t} = E_{F,i,t} + y_{error,i,t} \tag{21}$$

$$\psi(\alpha_{i,t}) = \int_{y_{i,t} \ge \alpha_{i,t}} \rho\left(y_{i,t}\right) dy \tag{22}$$

$\Psi(\alpha_{i,t})$ is the cumulative distribution function. Accordingly, the value at risk (VaR), which is the threshold of uncertain variable $y_{i,t}$ with confidence level $\beta$, is obtained in (23).

$$\mathrm{VaR}: \alpha_{\beta,i,t} = \max\left\{\alpha_{i,t} \in R : \psi\left(\alpha_{i,t}\right) \ge \beta\right\} \tag{23}$$

The corresponding CVaR value is represented as (24).

$$\Phi_{\beta i,t} = \frac{1}{1-\beta} \int_{y_{i,t} \le \alpha_{\beta i,t}} y_{i,t} \rho\left(y_{i,t}\right) dy_{i,t} = \alpha_{\beta i,t} - \frac{1}{1-\beta} \int_{y_{i,t} \in R^{m}} [\alpha_{\beta i,t} - y_{i,t}]^{+} \rho\left(y_{i,t}\right) dy_{i,t} \tag{24}$$

$$[Z]^{+} = \max\{0, Z\} \tag{25}$$

Then, the CVaR value can be obtained by optimizing $F()$ as in (26)-(27) [23]-[24]. By dispersing the integral part, $F()$ is further transformed into (28).

$$\max_{\alpha_{i,t} \in R} F_{\beta}(\alpha_{i,t}) = \Phi_{\beta,i,t} \tag{26}$$

$$F_{\beta}(\alpha_{i,t}) = \alpha_{i,t} - \frac{1}{1-\beta} \int_{y_{i,t} \in R^{m}} [\alpha_{i,t} - y_{i,t}]^{+} \rho\left(y_{i,t}\right) dy_{i,t} \tag{27}$$

$$F_{\beta}^{*}(\alpha_{i,t}) = \alpha_{i,t} - \frac{1}{M(1-\beta)} \sum_{k=1}^{M} [\alpha_{i,t} - y_{i,t,k}^{*}]^{+} \tag{28}$$

where $y_{i,t,k}^{*}$ is the $k$th sampling value of the uncertain variable $y_i$ at step $t$. Setting auxiliary variables $u_k = [\alpha_{i,t} - y_{i,t,k}^{*}]^{+}$, the CVaR value is obtained by solving an LP model (29). Finally, the CVaR value of RES-BSR $i$ at step $t$ is (30).

$$\max\left\{\alpha_{i,t} - \frac{1}{M(1-\beta)} \sum_{k=1}^{M} u_k\right\} \; s.t. \; u_k \ge 0, u_k \ge y_{i,t,k}^{*} - \alpha_{i,t} \tag{29}$$

$$P_{\mathrm{RE},i,t}^{\mathrm{CVaR}} = \max F_{\beta}^{*}(\alpha_{i,t}) \tag{30}$$

4) *Generator restart constraints*. Constraints for generator restart include critical time interval limit (31) and start up power requirement (32). Eq. (31) ensures that the restart time of NBSG $i$ is less than the critical maximum time interval or larger than the critical minimum time interval, and (32) ensures that NBSGs can only be restarted when the system can supply sufficient start-up power.

$$\begin{cases} u_{\mathrm{C},i} T_{\mathrm{C,min},i} \le t_{\mathrm{sta},i} \le M(1-u_{\mathrm{H},i}) T_{\mathrm{H,max},i} + u_{\mathrm{H},i} T_{\mathrm{H,max},i} \\ u_{\mathrm{C},i} + u_{\mathrm{H},i} = 1 \quad \forall i \in N_{\mathrm{NBS}} \end{cases} \tag{31}$$

$$\sum_{i \in N_{\mathrm{BS}} \bigcup N_{\mathrm{NBS}}} P_{\mathrm{G},i,t} + \sum_{i \in N_{\mathrm{RE}}} P_{\mathrm{RE},i,t}^{\mathrm{CVaR}} + \sum_{j \in N_{\mathrm{DS}}} P_{\mathrm{TB},j,t} \ge 0 \quad t = \{1,...,T\} \tag{32}$$

5) *Energization constraints*. Introducing binary variables $u_{\mathrm{bus},i,t}$, $u_{\mathrm{Line},l,t}$, $u_{\mathrm{bus},m,t}$ and $u_{\mathrm{bus},n,t}$. The correlated generator restart and bus and line energization status is presented in (33)-(35) [11]. Constraint (33) means NBSGs can be restarted and BSRs can supply power only after the energization of their respective bus $i$. The transmission line $l$ connects buses $n$ and $m$, and it cannot be energized at step $t$ when neither of the connected buses is energized (34). Constraint (35) means the transmission line $l$ can be energized one step after the energization of one of its connected buses.

$$\sum_{s \in \{1,2,3\}} O_{i,t}^{s} \le u_{\mathrm{bus},i,t} \quad \forall i \in N_{\mathrm{NBS}} \bigcup N_{\mathrm{BS}}, t = \{1,...,T\} \tag{33}$$

$$\begin{cases} u_{\mathrm{Line},l,t} \le u_{\mathrm{bus},m,t} \\ u_{\mathrm{Line},l,t} \le u_{\mathrm{bus},n,t} \end{cases} \forall l \in <m,n>, t = \{1,...,T\} \tag{34}$$

$$u_{\mathrm{Line},l,t+1} \le \left(u_{\mathrm{bus},m,t} + u_{\mathrm{bus},n,t}\right) \forall l \in <m,n>, t = \{1,...,T-1\} \tag{35}$$

### *B. Decentralized D-GSS optimization model of each DSO*

Because of the lack of power supply from the DS main substations, loads in DSs are normally shed after a partial or complete blackout [25]. For the sake of bulk system generator restart, the available DS power sources are used to provide power support to the TS after satisfying some critical loads. In

the generator restart process, part of loads are picked up for system power balance or critical load fast recovery requirement. Most of the rest un-served loads will be restored at later stages after the generator restart stage [4].

1) *Objective function*. The objective is to minimize the TD boundary mismatch penalty function of DS *j*.

$$\min \sum_{t=1}^{T}\left(v_{j,t}\left(P_{\mathrm{TB},j,t}-P_{\mathrm{DB},j,t}\right)+\left\|w_{j,t}\circ\left(P_{\mathrm{TB},j,t}-P_{\mathrm{DB},j,t}\right)\right\|_2^2\right)\ (j\in N_{\mathrm{SUB}}) \quad (36)$$

2) *DS operation model with configuration*. The multi-step DS network reconfiguration problem can be modeled as MISOCP (37)-(50). Constraints (37) and (38) represent the active and reactive power balance at node *m* of DS *j*, respectively. Constraint (39) means that the load will not be shed as long as it is reconnected. The voltage drop of branch *mn* at step *t* is calculated in (40). Constraint (41) calculates the current magnitudes of all branches and it is transformed to form the MISCOP model [26]. The voltage, current and TD boundary power limits are (42), (43) and (44), respectively. The spanning tree constraints (45)-(48) are required to ensure the radial topology of the DS [27]. Constraints (49)-(50) limit the number of switching actions of DS *j* in the restoration period *T*.

$$P_{\mathrm{G},m,t}-P_{\mathrm{DL},m,t}=\sum_{n\in N_{\mathrm{c}}(m)}\left(P_{mn,t}+I_{mn,t}^{\mathrm{sqr}}R_{mn}\right)-\sum_{n\in N_{\mathrm{p}}(m)}P_{nm,t} \quad m\in N_{sub,j} \quad (37)$$

$$Q_{\mathrm{G},m,t}-Q_{\mathrm{DL},m,t}=\sum_{n\in N_{\mathrm{c}}(m)}\left(Q_{mn,t}+I_{mn,t}^{\mathrm{sqr}}X_{mn}\right)-\sum_{n\in N_{\mathrm{p}}(m)}Q_{nm,t} \quad m\in N_{sub,j} \quad (38)$$

$$x_{\mathrm{L},m,t+1}\ge x_{\mathrm{L},m,t}\ \ t=\{1,...,T-1\},m\in N_{sub,j} \quad (39)$$

$$V_{m,t}^{\mathrm{sqr}}-V_{n,t}^{\mathrm{sqr}}=2\left(P_{mn,t}R_{mn}+Q_{mn,t}X_{mn}\right)+\left(R_{mn}^2+X_{mn}^2\right)I_{mn,t}^{\mathrm{sqr}} \quad m\in N_{sub,j},n\in N_{\mathrm{c}}(m) \quad (40)$$

$$V_{n,t}^{\mathrm{sqr}}I_{mn,t}^{\mathrm{sqr}}\ge P_{mn,t}^2+Q_{mn,t}^2 \quad m\in N_{sub,j},n\in N_{\mathrm{c}}(m) \quad (41)$$

$$V_{m,\min}^2\le V_{m,t}^{\mathrm{sqr}}\le V_{m,\max}^2 \quad m\in N_{sub,j} \quad (42)$$

$$0\le I_{mn,t}^{\mathrm{sqr}}\le Z_{j,mn,t}I_{mn,\max}^2 \quad m\in N_{sub,j},n\in N_{\mathrm{c}}(m) \quad (43)$$

$$-P_{\mathrm{DB},\max,j,t}\le P_{\mathrm{DB},j,t}\le P_{\mathrm{DB},\max,j,t} \quad j\in N_{\mathrm{SUB}} \quad (44)$$

$$\beta_{mn,t}+\beta_{nm,t}=Z_{j,mn,t} \quad m\in N_{sub,j},n\in N_{\mathrm{c}}(m),j\in N_{\mathrm{SUB}} \quad (45)$$

$$\sum_{n\in N_{\mathrm{p}}(m)}\beta_{mn,t}+\sum_{n\in N_{\mathrm{c}}(m)}\beta_{nm,t}=1 \quad \forall m\in\left\{2,...,\mathrm{N}_{sub,j}\right\} \quad (46)$$

$$\beta_{mn,t}=0 \quad m\in N_{sub,j}^{s},n\in N_{\mathrm{c}}(m) \quad (47)$$

$$0\le Z_{j,mn,t}\le 1 \quad m\in N_{sub,j},n\in N_{\mathrm{c}}(m),j\in N_{\mathrm{SUB}} \quad (48)$$

$$\sum_{t\in\{1,...,T-1\}}\sum_{m\in N_{sub,j}}\sum_{n\in N(m)}\alpha_{j,mn,t}\le C_j \quad (49)$$

$$\begin{cases}\alpha_{j,mn,t}\ge Z_{j,mn,t}-Z_{j,mn,t-1}\\ \alpha_{j,mn,t}\ge Z_{j,mn,t-1}-Z_{j,mn,t}\end{cases}\ m\in N_{sub,j}^{s},n\in N(m) \quad (50)$$

$N_{sub,j}$, $N_{\mathrm{p}}(m)$, $N_{\mathrm{c}}(m)$ and $N_{sub,j}^{s}$ are sets of nodes in DS *j*, parent nodes and child nodes of node *m*, and main substation node of DS *j*.

The exact convex relaxation of power flow equations requires: 1) the topology is radial, 2) the objective is convex, 3) the objective function is strictly increasing with the square of current, non-decreasing with the power injection and independent of the branch power flow, and 4) the problem is feasible [26]. Conditions 1), 2) and 4) are satisfied in the decentralized DS models, and 3) is satisfied if the loss function is added to the objective function. In order to maintain the realistic condition of the DS models, the sufficient condition 'no upper bounds on loads' is relaxed. Although the strict exactness proof is hard to be provided without the sufficient condition, the convex-relaxed equation (41) always converges to the original equality if the loss function is added to the objective function.

3) *RES-DG output assessment*. Similar to the TS RES-BSR output measurement, the CVaR value is used to represent uncertain RES-DG output.

$$F_{\beta}^{*}(\alpha_{m,t})=\alpha_{m,t}-\frac{1}{M(1-\beta)}\sum_{k=1}^{M}[\alpha_{m,t}-y_{m,t,k}^{*}]^{+}\ m\in N_{sub,j,\mathrm{RES}} \quad (51)$$

$$\max\left\{\alpha_{m,t}-\frac{1}{M(1-\beta)}\sum_{k=1}^{M}u_k\right\}\ s.t.\ u_k\ge 0,u_k\ge y_{m,t,k}^{*}-\alpha_{m,t} \quad (52)$$

$$P_{\mathrm{G},m,t}=P_{\mathrm{DG},m,t}^{\mathrm{CVaR}}=\max F_{\beta}^{*}(\alpha_{m,t})\ m\in N_{sub,j,\mathrm{RES}} \quad (53)$$

where $y_{m,t,k}^{*}$ is the *k*th sampling value of the uncertain variable $y_m$ at step *t*, $\alpha_{m,t}$ is the threshold variable of RES-DG node *m* at step *t* and auxiliary variables $u_k=[\alpha_{m,t}-y_{m,t,k}^{*}]^{+}$. $N_{sub,j,\mathrm{RES}}$ is the set of RES-DG connected nodes in DS *j*. The CVaR value of RES-DG power supply connected at node *m* at step *t* is (53).

4) *ES model*. With reliable and flexible power supply ability, ESs in the DS are useful BSRs. According to [13], the ES model is described by (54)-(59). Depending on the operation mode, constraints (54)-(55) represent the charging/discharging limits. Constraint (57) guarantees that the ES works in only one mode at step *t*. The state of charge (SOC) of the ES is (58), and (59) is the SOC limit.

$$-P_{\mathrm{CH},m,\max}x_{\mathrm{CH},m,t}\le P_{\mathrm{CH},m,t}\le 0\ m\in N_{sub,j,\mathrm{ES}},t=\{1,...,T\} \quad (54)$$

$$0\le P_{\mathrm{DC},m,t}\le P_{\mathrm{DC},m,\max}x_{\mathrm{DC},m,t} \quad m\in N_{sub,j,\mathrm{ES}},t=\{1,...,T\} \quad (55)$$

$$x_{\mathrm{CH},m,t}+x_{\mathrm{DC},m,t}\le 1\ m\in N_{sub,j,\mathrm{ES}},t=\{1,...,T\} \quad (56)$$

$$E_{\mathrm{ES},m,t}=E_{\mathrm{ES},m,t-1}-\Delta T\left(P_{\mathrm{DC},m,t}\lambda_{\mathrm{DC},m}^{-1}+P_{\mathrm{CH},m,t}\lambda_{\mathrm{CH},m}\right)/C_{\mathrm{ES},m} \quad m\in N_{sub,j,\mathrm{ES}},\ t=\{1,...,T\} \quad (57)$$

$$0\le E_{\mathrm{ES},m,t}\le E_{\mathrm{ES},m,\max}\ m\in N_{sub,j,\mathrm{ES}},\ t=\{1,...,T\} \quad (58)$$

$$P_{\mathrm{G},m,t}=P_{\mathrm{ES},m,t}\ m\in N_{sub,j,\mathrm{ES}} \quad (59)$$

where $N_{sub,j,\mathrm{ES}}$ is the set of ES nodes in DS *j*.

5) *Boundary constraint*. For the main station of each DS, (60) is required to maintain the coupling of the TS and DS *j*.

$$P_{\mathrm{G},m,t}=-P_{\mathrm{DS},j,t}\ t=\{0,...,T\},m\in N_{sub,j} \quad (60)$$

Note that the DS model is built for the multi-step process where step $t\in\{1,\ldots,T\}$.

## IV. Solution Method for Decentralized D-GSS Models

This section introduces the iterative calculation process to solve the decentralized D-GSS models. The P-ATC algorithm is developed to handle the integrated binary variables as well as simplify decentralized models. The D-GSS scheme can be obtained by iteratively solving the TS MIQP model, DS QP models and projection functions.

### A. Iterative calculation process of P-ATC algorithm

Fig. 5 is the flowchart of the calculation process of the proposed method. Reliable power supplies of uncertain RESs are assessed first and are used in the iterative calculation process. The iterative calculation process of the developed P-ATC algorithm aims to decouple the decentralized models and solve the proposed D-GSS problem.

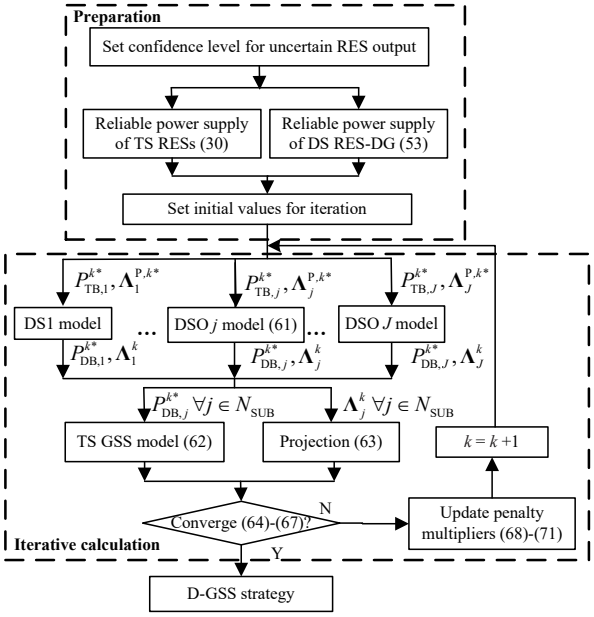


Fig. 5. Flowchart of calculation process

The projection method for the distributed algorithm is used to develop the P-ATC algorithm. Accordingly, extra binary variables $\boldsymbol{\Lambda}^{\mathrm{P}}_{j,t} = [x^{\mathrm{P}}_{\mathrm{L},m,t}, \alpha^{\mathrm{P}}_{j,mn,t}, \beta^{\mathrm{P}}_{mn,t}, x^{\mathrm{P}}_{\mathrm{CH},m,t}, x^{\mathrm{P}}_{\mathrm{DC},m,t}]$ are introduced for DS models, and the original binary variables $\boldsymbol{\Lambda}_{j,t} = [x_{\mathrm{L},m,t}, \alpha_{j,mn,t}, \beta_{mn,t}, x_{\mathrm{CH},m,t}, x_{\mathrm{DC},m,t}]$ are transformed to continuous variables. The detailed iterative calculation is described as follows.

*Step* 0: Set the iteration number $k$=1. Define the values of $P^{k*}_{\mathrm{TS},j}$, $v^{k}_{j}$, $w^{k}_{j}$, $v^{\mathrm{P},k}_{j}$ and $w^{\mathrm{P},k}_{j}$ for the first iteration.

*Step* 1: Solve the DS models in (61) in parallel with fixed $P^{k*}_{\mathrm{TS},j,t}$ obtained from the last iteration. Obtain $P^{k}_{\mathrm{DS},j}$ and $\boldsymbol{\Lambda}^{k}_{j}$.

$$\begin{aligned}\min\ & v^{k}_{j}\left(P^{k*}_{\mathrm{TB},j} - P^{k}_{DB,j}\right) + \left\| w^{k}_{j} \circ \left(P^{k*}_{\mathrm{TB},j} - P^{k}_{\mathrm{DB},j}\right)\right\|^{2}_{2} \\ & + \boldsymbol{v}^{\mathrm{P},k}_{j}\left(\boldsymbol{\Lambda}^{\mathrm{P},k*}_{j} - \boldsymbol{\Lambda}^{k}_{j}\right) + \left\| \boldsymbol{w}^{\mathrm{P},k}_{j} \circ \left(\boldsymbol{\Lambda}^{\mathrm{P},k*}_{j} - \boldsymbol{\Lambda}^{k}_{j}\right)\right\|^{2}_{2} \\ s.t.\ & (36)-(60) \\ & \boldsymbol{\Lambda}^{k}_{j} \in [0,1] \\ & \boldsymbol{\Lambda}^{k}_{j} = [\Lambda^{k}_{j,0}, ..., \boldsymbol{\Lambda}^{k}_{j,t}, ..., \boldsymbol{\Lambda}^{k}_{j,T}] \\ & \boldsymbol{\Lambda}^{\mathrm{P},k*}_{j} = [\Lambda^{\mathrm{P},k*}_{j,0}, ..., \boldsymbol{\Lambda}^{\mathrm{P},k*}_{j,t}, ..., \boldsymbol{\Lambda}^{\mathrm{P},k*}_{j,T}]\end{aligned} \tag{61}$$

*Step* 2: Solve the TS model (62) with fixed $P^{k*}_{\mathrm{DS},j}$ ($\forall j \in N_{\mathrm{SUB}}$) obtained from the last iteration, and get $P^{k+1*}_{\mathrm{TS},j}$ for $k$+1*th* iteration of the DS models.

$$\begin{aligned}\min\ & \sum_{i \in N_{\mathrm{NBR}}} \left(P^{\max}_{\mathrm{G},i} - P^{\mathrm{crk}}_{\mathrm{G},i}\right) t_{\mathrm{sta},i} \\ & + \sum_{j \in N_{\mathrm{SUB}}} \left( \nu_{j}\left(P^{k}_{\mathrm{TB},j} - P^{k*}_{\mathrm{DB},j}\right) + \left\| w_{j} \circ \left(P^{k}_{\mathrm{TB},j} - P^{k*}_{\mathrm{DB},j}\right)\right\|^{2}_{2} \right) \\ s.t.\ & (5)-(17), (19)-(20), (28)-(35)\end{aligned} \tag{62}$$

*Step* 3: Update binary variables using the projection function (63).

$$\boldsymbol{\Lambda}^{\mathrm{P},k+1}_{j} = \Pi\left(\boldsymbol{\Lambda}^{k}_{j}\right)\ (\forall j \in N_{\mathrm{SUB}}) \tag{63}$$

where $\Pi$ represents the projection onto variables $\boldsymbol{\Lambda}^{\mathrm{P},k}_{j}$, which means $\Pi$ round the argument to its nearest binary value.

*Step* 4: Check the necessary-consistency condition (64)-(65) and sufficient condition (66) where $f$ represents the summary of objective values of the TS and DS models. If they are satisfied or the iteration limit (67) is reached, the final result is obtained and the solution procedure stops, otherwise, proceed to *step* 5.

$$\left|P^{k+1}_{\mathrm{TB},j} - P^{k}_{\mathrm{DB},j}\right| \le \sigma_{1}\ \forall j \in N_{\mathrm{SUB}} \tag{64}$$

$$\left\|\boldsymbol{\Lambda}^{\mathrm{P},k*}_{j} - \boldsymbol{\Lambda}^{k*}_{j}\right\| \le \sigma_{2} \wedge \left\|\boldsymbol{\Lambda}^{\mathrm{P},k+1*}_{j} - \boldsymbol{\Lambda}^{\mathrm{P},k*}_{j}\right\| \le \sigma_{3}\ \forall j \in N_{\mathrm{SUB}} \tag{65}$$

$$\left|(f^{k}_{i} - f^{k-1}_{i})/f^{k}_{i}\right| \le \sigma_{4}\ \ \forall i \in N_{\mathrm{SUB}} \vee i \in \mathrm{TS} \tag{66}$$

$$k \le K \tag{67}$$

*Step* 5: Update penalty parameters $v^{k}_{j}$, $w^{k}_{j}$, $v^{\mathrm{P},k}_{j}$ and $w^{\mathrm{P},k}_{j}$ according to (68)-(71) [28]. Set $k$=$k$+1 and go to *step* 1.

$$\boldsymbol{v}^{k+1}_{j} = \boldsymbol{v}^{k}_{j} + 2\left(\boldsymbol{w}^{k}_{j}\right)^{2}\left(P^{k+1}_{\mathrm{TB},j} - P^{k}_{\mathrm{DB},j}\right) \forall j \in N_{\mathrm{SUB}} \tag{68}$$

$$\boldsymbol{w}^{k+1}_{j} = \beta \boldsymbol{w}^{k}_{j}\left(\beta \ge 1\right) \quad \forall j \in N_{\mathrm{SUB}} \tag{69}$$

$$\boldsymbol{v}^{\mathrm{P},k+1}_{j} = \boldsymbol{v}^{\mathrm{P},k}_{j} + 2\left(\boldsymbol{w}^{\mathrm{P},k}_{j}\right)^{2}\left(\boldsymbol{\Lambda}^{\mathrm{P},k}_{j} - \boldsymbol{\Lambda}^{k}_{j}\right) \forall j \in N_{\mathrm{SUB}} \tag{70}$$

$$\boldsymbol{w}^{\mathrm{P},k+1}_{j} = \beta^{\mathrm{P}} \boldsymbol{w}^{\mathrm{P},k}_{j}\left(\beta^{\mathrm{P}} \ge 1\right) \quad \forall j \in N_{\mathrm{SUB}} \tag{71}$$

In this algorithm, the TS model (62) is a MIQP, and the DS model (61) is a second-order conic program (SOCP).

The projection function based decentralized algorithm is originally proposed for the fast calculation of the integer variable integrated models [21].The projection method replaces binary variables with continuous ones in [0, 1], and the iterative calculation process uses the continuous variables to provide binary results by ensuring very small distance between binary variables and the corresponding continuous variables. In the proposed algorithm above, the DS model (61) is transformed from a MISOCP into a SOCP using the projection method. The transformation largely reduces the computational complexity of the DS multi-step network reconfiguration models. Moreover, although the calculated models are with continuous variables, the consistency condition (65) ensures the related part of the convergent result is binary.

The proposed P-ATC method has good convergence characteristic for the D-GSS problem in this paper. The iterative process of the proposed P-ATC method is a *method of multipliers* [28] which includes quadratic penalty terms in the objective functions as a local convexifier. With the increase of the iteration number, the values of penalty multipliers grow according to (69) and (71) and the 'convexity' is enhanced to improve the convergence of the iteration process. A feasible solution without any constraint violations can be obtained as long as the iterative process converges. Normally, a small optimality gap exists when the original model is a MILP and the decentralized ones are MIQPs.

## V. Case Study

Two test systems were used to validate the effectiveness of

the proposed scheme, the T6D2 [15] and the T118D5 system, described next. The parameter $\beta$ is set as 1.1 and the residuals $\sigma_1$, $\sigma_2$, $\sigma_3$ and $\sigma_4$ are set as 0.1%. Samples of uncertain outputs of RES based sources are obtained using beta distribution with the standard variance 13.82%. Confidence levels are set as 95% without special explain. All case studies were conducted using CPLEX V12.8.0 on a computer with the Intel(R) Core(TM) i5-2400 CPU and 4 GB RAM. The case studies mainly demonstrate the acquisition and performance of the decentralized D-GSS scheme. The transmission path is found according to the determined GSS, i.e. without influencing the feasibility of the proposed method, the transmission path can be selected according to the feasible shortest path from BSRs to NBSRs [7], [12]. The time step for the generator restart is set as 10 min containing transmission path energization in the beginning 5 min..

### *A. Iteration process of P-ATC based calculation and efficiency of D-GSS scheme*

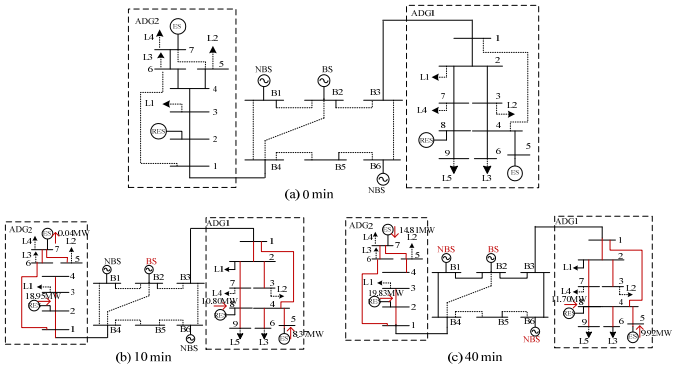


Fig. 6. The D-GSS scheme with T6D2 system

Fig. 6 (a) shows the T6D2 test system which consists of a 6 bus TS and two DSs. There are a RES-DG and an ES in each DS that can be used as BSRs. The critical loads connected to bus 2 and bus 6 in DS1 are required to be restored before step 2 and step 3, respectively. Using the LP model of the CVaR method, the reliable power supplies of RES-DGs are 12 MW in DS1s and 20 MW in DS2 with a confidence level of 95%.

The D-GSS scheme utilizes available power sources both in the TS and DSs to help restart NBSRs. Fig. 6 (b)-(c) show the actions taken at the DSs regarding RES-DG outputs, ES charge or discharge power and branch switching to benefit the GSS of the TS. Meanwhile, DS security operation constraints and the required critical load pickup should be satisfied. Fig. 7 shows the iteration process of the TD boundary powers. In a decentralized way, the TSO makes GSS decisions and sends boundary power demands ($P_{\mathrm{TB},1}$ and $P_{\mathrm{TB},2}$) to DSOs considering the available power supplies from the DS, while DSOs submit available boundary power supplies ($P_{\mathrm{DB},1}$ and $P_{\mathrm{DB},2}$) to the TSO considering the TSO power demand and their regional grid operation conditions. In the process, the penalty function of objectives make $P_{\mathrm{TB},1}$ and $P_{\mathrm{TB},2}$ in the TS and $P_{\mathrm{DB},1}$ and $P_{\mathrm{DB},2}$ in DSs get closer and finally converge at each time step.

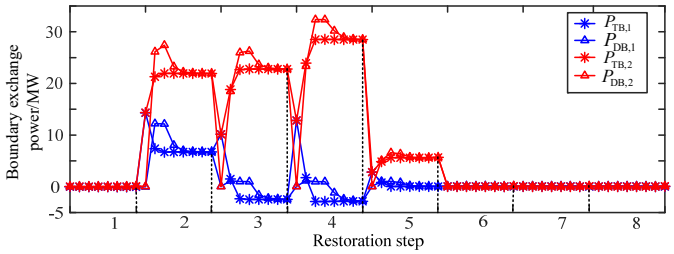


Fig. 7. TD boundary power iteration process in eight restoration steps

For the GSS problem, [7] provides the classic MILP model using available resources at the TS level, and [12] builds a centralized optimization model considering assistances from micro-grids. Based on the former studies, three schemes were simulated to show the efficiency of the proposed scheme: 1) the proposed decentralized D-GSS scheme; 2) the centralized DS assisted GSS scheme (C-GSS) [12]; and 3) the conventional TS GSS scheme, i.e. without the assistance of DSs (T-GSS) [7].

Table I shows the efficiency of the three schemes. The last column shows the start-up sequence of generators connected to B1, B2 and B6. As shown, the MILP model based T-GSS scheme is very fast, however, the obtained GSS result has a much higher objective function value which means much less generation capacity during the restoration process. Consequently, the restoration will be delayed. With the assistance of DSs, the model of the C-GSS scheme is a coupled TS and DS MISOCP model considering TS GSS and DS multi-step operation with reconfiguration, while the D-GSS scheme contains decoupled TS MIQP model and DS SOCP models. Compared with the C-GSS scheme, the P-ATC based D-GSS shows higher efficiency with much reduced computation time and practically the same GSS result.

TABLE I
EFFICIENCIES OF DIFFERENT SCHEME

| Scheme | Cal_time (s) | Obj_val (MW) | GSS (step) |
|---|---|---|---|
| D-GSS | 9.75 | 206.04 | [2 1 2] |
| C-GSS [12] | 630.91 | 206.00 | [2 1 2] |
| T-GSS [7] | 0.41 | 486.00 | [6 1 2] |

The uncertain RES based BSRs impact the GSS by their reliable power supply which is determined by the integrated amount and confidence level. With the same RES-DG integration amount (RES1 and RES2) in DS1 and DS2, the restart of NBSG are delayed when the confidence level become higher. That is because a higher confidence level leads to a higher reliability requirement of power supply of uncertain RES sources. As such, the available power supply from RES-BSRs is less and the restart of NBSG needs to wait for the ramping up of traditional BSGs. On the other side, under confidence level 95%, the increase of RES integration makes the generator restart in earlier steps, which means a better GSS scheme. Note that the benefit is not unlimited for the GSS problem. The ideal GSS for a system is that BSGs restart at the first step and all the other NBGSs restart at the second step. Therefore, the GSS scheme [2 1 2], which represents generators connected to B1, B2 and B6 restart at the second, first and second step, is kept although available power supply increases with a larger RES integration amount.

TABLE II
INFLUENCE OF UNCERTAIN RES BASED BSRS

| Confidence level | RES1 (MW) | RES2 (MW) | GSS (step) |
|---|---|---|---|
| 95% | 27 | 45.15 | [2 1 2] |
| 99.5% | 27 | 45.15 | [3 1 2] |
| 99.7% | 27 | 45.15 | [4 1 2] |
| 99.99% | 27 | 45.15 | [4 1 2] |
| 95% | 33.95 | 56.58 | [2 1 2] |
| 95% | 24.61 | 41.16 | [2 1 2] |
| 95% | 17.06 | 28.57 | [3 1 2] |
| / | 0 | 0 | [5 1 2] |

### *B. Computation efficiency and GSS performance of D-GSS scheme with large system*

The T118D5 system consists of an IEEE 118-bus TS system and five IEEE 123-bus DSs. DSs are connected to buses 27, 54, 74, 90 and 112 of the TS system. At the TS level, five wind farms are connected to buses 18, 32, 56, 77 and 116. At the DS level, two RES-DGs are connected to buses 85 and 104, and an ES is connected to bus 39 in each DS. The computation efficiency of the developed P-ATC method is compared with the original ATC method [16]. Moreover, the performance of the decentralized D-GSS scheme is compared with the C-GSS scheme [12] and T-GSS scheme [7].

Fig. 8 shows the iteration processes of the P-ATC and ATC methods in the multi-step restoration process. In order to respect the generator restart characteristics, related models are constructed with 25 restoration steps. It is shown that the ATC method satisfies the required 0.1% converge threshold after 25 iterations, while the P-ATC method needs 12 iterations. Although both methods converge and are able to realize the decentralized D-GSS scheme, the P-ATC method is much more efficient computationally requiring 56.52 s compared with 43,943.45 s of the ATC. This computation time reduction is mainly due to the processing of integer variables using the P-ATC method. Namely, for the DS models containing 25 restoration steps, the ATC method iteratively performs MISOCPs, while the P-ATC method performs SOCPs. This makes decentralized models much easier to solve.

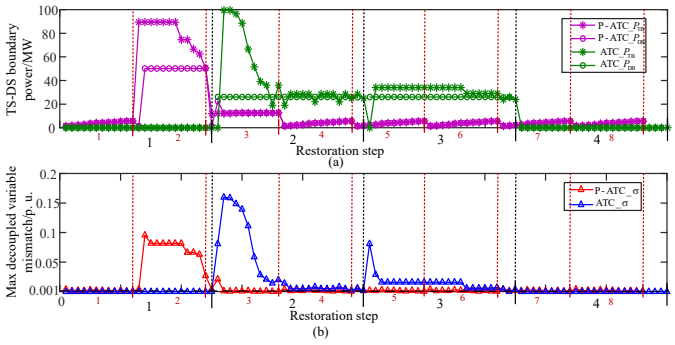


Fig. 8. Multi-step iteration process of P-ATC/ATC based TD boundary power condition (a) and maximal decoupled variables mismatch (b)

In addition, the P-ATC method finds a better GSS scheme. Both of the methods can restart all the generators in 4 steps. However, as shown by 'P-ATC_$P_{TD}$' and 'ATC_$P_{TD}$' in Fig. 8 (a), the P-ATC method utilizes larger amount of power supply from DSs at step 2 than the ATC one. Consequently, as shown in Fig. 9, the P-ATC method restarts three more NBSGs at step 2 and further restarts extra two NBSGs at step 3. More generators can be restarted earlier based on the P-ATC method. Thus in the same system and under the same BSR conditions, the P-ATC method achieves better utilization of the additional power support from DS for generator restart compared with the ATC one.

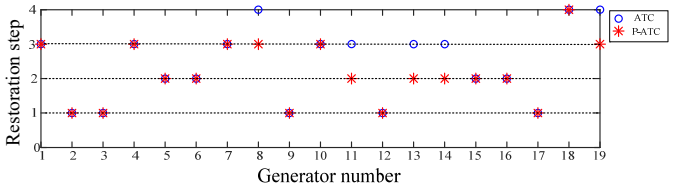


Fig. 9. Generator restart conditions of different methods

The GSS performance of the three schemes is shown in Fig. 10. The P-ATC based decentralized D-GSS scheme shows similar system generation capability (GC) compared with the centralized C-GSS scheme (0.37% generation difference in the whole process). The conventional T-GSS scheme performs worse, since less GC is available at each step. It should be noted that the C-GSS scheme may not be applicable in real DS assisted GSS process because detailed system information of DSOs is not normally available to the TSO. For the generator restart problem, extra power support is needed especially at early restoration stages, when the system has power deficiency, e.g., steps 2-3 in Fig. 10. Since tens MW of power supply can normally restart a generator of hundreds MW capability, little power support at early steps helps the system obtain much more generation at later steps. It should be noted that although the reliable power supply of RES-DGs and ESs at the DS level may be with a small amount, their use in early steps can largely enhance the GC during the whole restoration process. Therefore, the proposed decentralized D-GSS scheme improves the generator restart process by timely power support in the early stages.

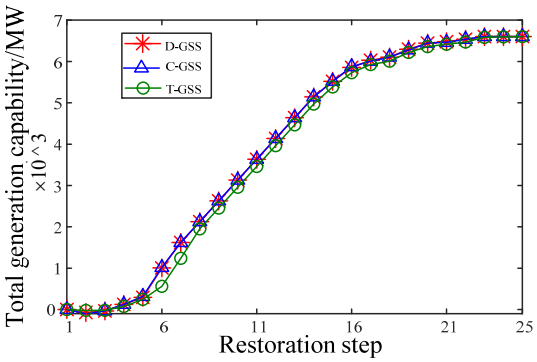


Fig. 10. Generator capacity conditions of different schemes

## VI. CONCLUSION

This paper proposes a new decentralized bulk system GSS scheme with the assistance of DSs. The decentralized D-GSS strategy is obtained based on the developed P-ATC algorithm. With the proposed scheme, available BSRs in the DS are utilized to realize better GSS with more available generation during the restoration process. Moreover, the independent decision-making of the TSO and DSOs are maintained. By applying the proposed P-ATC algorithm, the optimal D-GSS result is obtained by iteratively solving the MISOCP model of the TSO, parallel SOCP models of DSOs and projection functions for binary variables. The case study results show the computa-

tional efficiency of the decentralized D-GSS scheme without loss of optimality. The decentralized D-GSS scheme benefits the restoration process with power support from DSs at early restoration stages.

The future work can be focused on considering the fault isolation of DSs, and the D-GSS scheme can be developed with unbalanced DSs. Moreover, based on the idea of decentralized coordination, other problems in bulk system restoration process can be studied considering the assistance from DSs.

## REFERENCES


[1] F. Qiu and P. Li, "An integrated approach for power system restoration planning," *Proc. IEEE*, vol. 105, no. 7, pp. 1234-1252, 2017.

[2] M. Panteli, D. N. Trakas, P. Mancarella, and N. D. Hatziargyriou, "Power systems resilience assessment: hardening and smart operational enhancement strategies," *Proc. IEEE*, vol. 105, no. 7, pp. 1202-1213, 2017.

[3] F. Qiu, J. Wang, C. Chen, and J. Tong, "Optimal black start resource allocation," *IEEE Trans. Power Syst*., vol. 31, no. 3, pp. 2493–2494, 2016.

[4] L. H. Fink, K. L. Liou, and C. C. Liu, "From generic restoration actions to specific restoration strategies," *IEEE Trans. Power Syst*., vol. 10, no. 2, pp. 745–751, 1995.

[5] G. Patsakis, D. Rajan, I. Aravena, J. Rios and S. Oren, "Optimal black start allocation for power system restoration," *IEEE Trans. Power Syst*., vol. 33, no. 6, pp. 6766–6776, 2018.

[6] C.-C. Liu, K.-L. Liou, R. F. Chu, and A. T. Holen, "Generation capability dispatch for bulk power-system restoration: A knowledge based approach," *IEEE Trans. Power Syst*., vol. 8, no. 1, pp. 316–325, 1993.

[7] W. Sun, C.-C. Liu, and L. Zhang, "Optimal generator start-up strategy for bulk power system restoration," *IEEE Trans. Power Syst*., vol. 26, no. 3, pp. 1357–1366, 2011.

[8] L. Sun, Z. Lin, Y. Xu, F. Wen, C. Zhang and Y. Xue, "Optimal skeleton-network restoration considering generator start-up sequence and load pickup," *IEEE Trans. Smart Grid*, vol. 10, no. 3, pp. 3174-3185, 2019.

[9] W. Sun, C. C. Liu and S. Liu, "Black start capability assessment in power system restoration," *IEEE PES Generl Meeting*, pp. 1-7, 2011.

[10] L. Sun, C. Peng, J. Hu and Y. Hou, "Application of type 3 wind turbines for system restoration," *IEEE Trans. Power Syst*., vol. 33, no. 3, pp. 3040-3051, 2018.

[11] A. Golshani, W. Sun, Q. Zhou, Q. P. Zheng, J. Wong and F. Qiu, "Coordination of wind farm and pumped-storage hydro for a self-healing power grid," *IEEE Trans. Sustain. energy*, vol. 9, no. 4, pp. 1910-1920, 2018.

[12] Y. Zhao, Z. Lin, Y. Ding, Y. Liu, L. Sun and Y. Yan, "A model predictive control based generator start-up optimization strategy for restoration with microgrids as black-start resources," *IEEE Trans. Power Syst*., vol. 33, no. 6, pp. 7189-7203, 2018.

[13] Z. Wang and J. Wang, "Self-healing resilient distribution systems based on sectionalization into microgrids," *IEEE Trans. Power Syst*., vol. 30, no. 6, pp. 3139-3149, 2015.

[14] J. Zhao, H. Wang, Y. Liu, Q. Wu, Z. Wang and Y. Liu, "Coordinated restoration of transmission and distribution system using decentralized scheme," *IEEE Trans. Power Syst*., vol. 34, no. 5, pp. 3428-3442, 2019.

[15] Z. Li, Q. Guo, H. Sun, and J. Wang, "Coordinated economic dispatch of coupled transmission and distribution systems using heterogeneous decomposition," *IEEE Trans. Power Syst*., vol. 31, no. 6, pp. 4817–4830, 2016.

[16] A. Kargarian and Y. Fu, "System of systems based security-constrained unit commitment incorporating active distribution grids," *IEEE Trans. Power Syst*, vol. 29, no. 5, pp. 2489–2498, 2014.

[17] C. Qi, K. Wang, Y. Fu, G. Li, B. Han, R. Huang and T. Pu, "A decentralized optimal operation of AC/DC hybrid distribution grids," *IEEE Trans. Smart Grid*, vol. 9, no. 6, pp. 6095-6105, 2018.

[18] M. Cui, J. Wang, and B. Chen, "Flexible machine learning-based cyberattack detection using spatiotemporal patterns for distribution systems," *IEEE Trans. on Smart Grid*, vol. 11, no. 2, pp. 1805–1808, 2020.

[19] S. Huang, Q. Wu, Y. Guo, X. Chen, B. Zhou and C. Li, "Distributed voltage control based ADMM for large-scale wind farm cluster connected to VSC-HVDC," *IEEE Trans. Sustain. Energy*, vol. 11, no. 2, pp. 584-594, 2019.

[20] S. Huang, Q. Wu, J. Zhao, W. Liao, "Distributed optimal voltage control for VSC-HVDC connected large-scale wind farm cluster based on analytical target cascading method," *IEEE Trans. Sustain. Energy*, 2019, in press.

[21] R. Takapoui, N. Moehle, S. Boyd and A. Bemporad, "A simple effective heuristic for embedded mixed-integer quadratic programming," in *Proc. American Control Conf*., Boston, Massachusetts, pp. 5619–5625, 2016.

[22] G. Monique and S. Kim, "Lagrangean decomposition: A model yielding stronger Lagrangean bounds," *Math. Program*., vol. 39, no. 2, pp. 215-228, 1987.

[23] R. T. Rockafellar and S. Uryasev, "Optimization of conditional value-atrisk," *J. risk*, vol. 2, pp. 21-42, 1999.

[24] P. Krokhmal, J. Palmquist and S. Uryasev, "Portfolio optimization with conditional value-at-risk objective and constraints", *J. risk*, vol. 4, pp. 43-68, 2002.

[25] National Grid ESO LFDD report. 2019, [Online]. Available: https://www.nationalgrideso.com/document/151081/download

[26] M. Farivar and S. H. Low, "Branch flow model: relaxations and convexification - part I," *IEEE Trans. Power Syst*., vol. 28, no. 3, pp. 2554–2564, 2013.

[27] S. Lei, C. Chen, Y. Song and Y. Hou, "Radiality constraints for resilient reconfiguration of distribution systems: Formulation and application to microgrid formation," *Trans. Smart Grid*, early access.

[28] S. Tosserams, L. F. P. Etman, P. Y. Papalambros, and J. E. Rooda, "An augmented Lagrangian relaxation for analytical target cascading using the alternating directions method of multipliers," *Struct. Multidisc Optim.*, vol. 31, no. 3, pp. 176–189, 2006